Electronic Supplementary Material (ESI) for New Journal of Chemistry.
This journal is © The Royal Society of Chemistry and the Centre National de la Recherche Scientifique 2018

Flexible yolk-shelled $NiCo_2S_4$ hollow spheres/RGO film electrodes for efficient supercapacitive energy storage

*Yilin Wu[a], Ming Yan[a], Lin Sun[b], Weidong Shi[b,]**

[a]*Institute of Green Chemistry and Chemical Technology, School of Chemistry and Chemical Engineering, Jiangsu University, Zhenjiang 212013, China*

[b]*School of Chemistry and Chemical Engineering, Jiangsu University, Zhenjiang 212013, China*

*Corresponding Author**

E-mail: wuyilin@ujs.edu.cn; swd1978@ujs.edu.cn

Telephone Number: +86 0511-88790683; Fax: +86 0511-88791800

Formation of ball-in-ball hollow spheres.

As shown in Fig. S1., we develop a hydrothermal method to prepare uniform nickel cobalt glycerate (NiCo-glycerate) spheres as the precursor. A solution sulfidation process under solvothermal condition is then utilized to convert the NiCo-glycerate solid precursors into yolk-shelled $NiCo_2S_4$ hollow spheres. The whole formation process can be generally divided into two stages as schematically. At stage I, sulfide (S^{2-}) ions released from the decomposition of TAA at high temperature react with metal ions on the surface of NiCo-glycerate and produce NiCo-glycerate@$NiCo_2S_4$ core-shell structure. This sulfidation process can be described as an anion exchange reaction of the NiCo-glycerate. Further reaction between the inward diffused S^{2-} ions and faster outward diffused metal cations supplies the growth of the $NiCo_2S_4$ shell and leads to a well-defined gap between the shell and the NiCo-glycerate core. When the reaction proceeds to certain degree, it will be more difficult for the metal cations to diffuse to the outer shell through the enlarged empty gap. Thus, a secondary $NiCo_2S_4$ shell would be formed on the remaining core as shown at stage II. On the completion of the anion exchange reaction, unique yolk-shelled $NiCo_2S_4$ hollow spheres are obtained at the end.

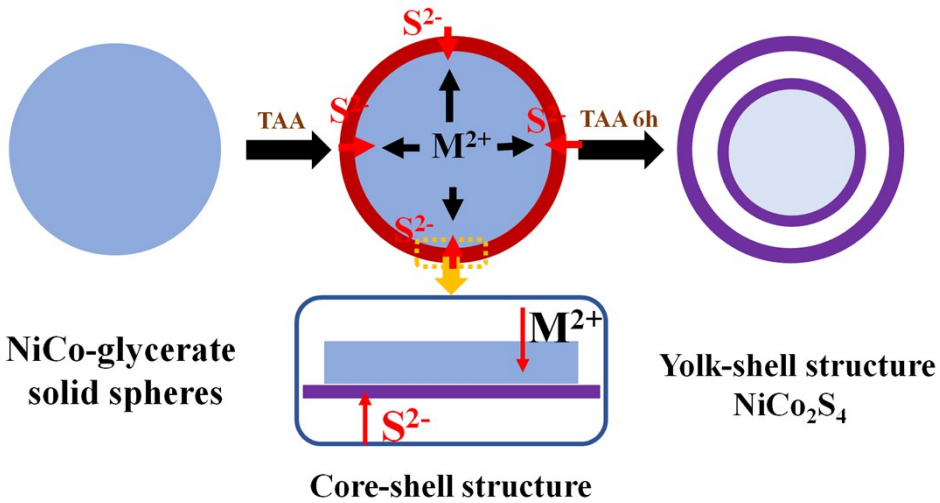

Fig. S1. schematic illustration of the formation process of yolk-shelled $NiCo_2S_4$ hollow spheres

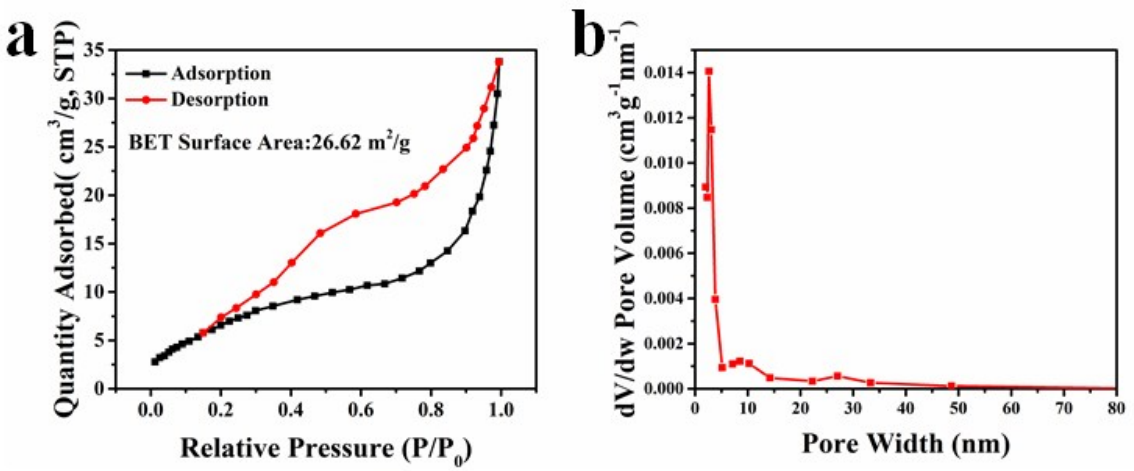

Fig. S2. Nitrogen adsorption and desorption isotherm of the $NiCo_2S_4$/2RGO composite (a), the pore size distribution curve (b).

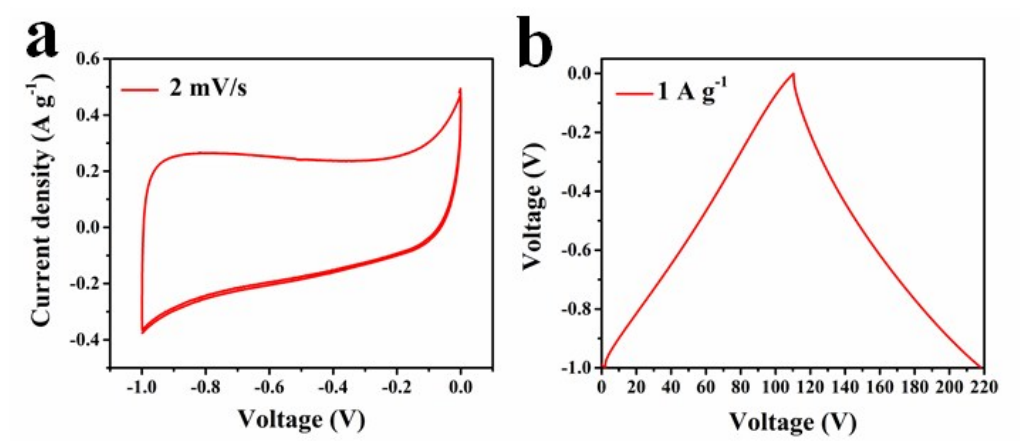

Fig. S3. CV curves of AC at 2 mV/s (a); GCD of AC at 1 Ag^{-1} (b).

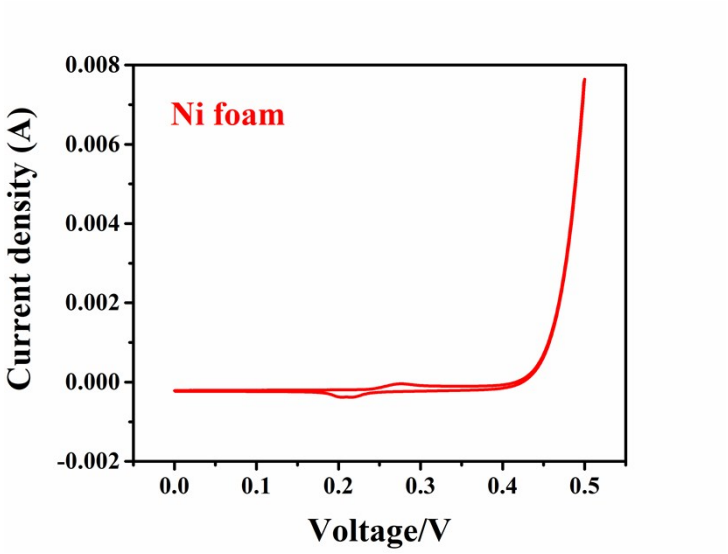

Fig. S4. CV curves of as-prepared Ni foam sample at the scan rates of 2 mV/s.

Table S1. Supercapacitor performances based on $NiCo_2S_4$ materials presented in literature and the present work.

Materials	[a]C_{max}	[b]T	[c]$C_m\%_T$	Ref.
$NiCo_2S_4$ nanoboxes	777.0 F g^{-1} (4 A g^{-1})	5000	75.0%	[45]
$NiCo_2S_4$ nanoplates	437.0 F g^{-1} (1 A g^{-1})	1000	81.0%	[46]
$NiCo_2S_4$@graphene	1432.0 F g^{-1} (1 A g^{-1})	5000	84.3%	[47]
$NiCo_2S_4$@rGO@CNT	1242.5 F g^{-1} (2 A g^{-1})	2000	53.9%	[48]
$NiCo_2S_4$/2RGO films	1000.5 F g^{-1} (1 A g^{-1})	5000	80.5%	This work

[a]C_{max}, maximum specific capacitance,
[b]T, cycles of cycle life test,
[c]C_m%, retention rate of specific capacitance after cycle life test.